

Supplementary Information for

Circular RNA circRILPL1 promotes nasopharyngeal carcinoma malignant progression

by activating the Hippo-YAP signaling pathway

Authors

Pan Wu^{1,2}, Xiangchan Hou^{1,2}, Miao Peng^{1,2}, Xiangying Deng^{1,2}, Qijia Yan⁴, Chunmei Fan^{1,2},

Yongzhen Mo^{1,2}, Yuming Wang^{2,3}, Zheng Li², Fuyan Wang², Can Guo², Ming Zhou², Qianjin

Liao¹, Hui Wang¹, Zhaoyang Zeng^{1,2}, Weihong Jiang³, Guiyuan Li^{1,2}, Wei Xiong^{1,2}, Bo

Xiang^{1,2*}

***Corresponding author**

Bo Xiang, xiangbolin@csu.edu.cn,

Fig. S1

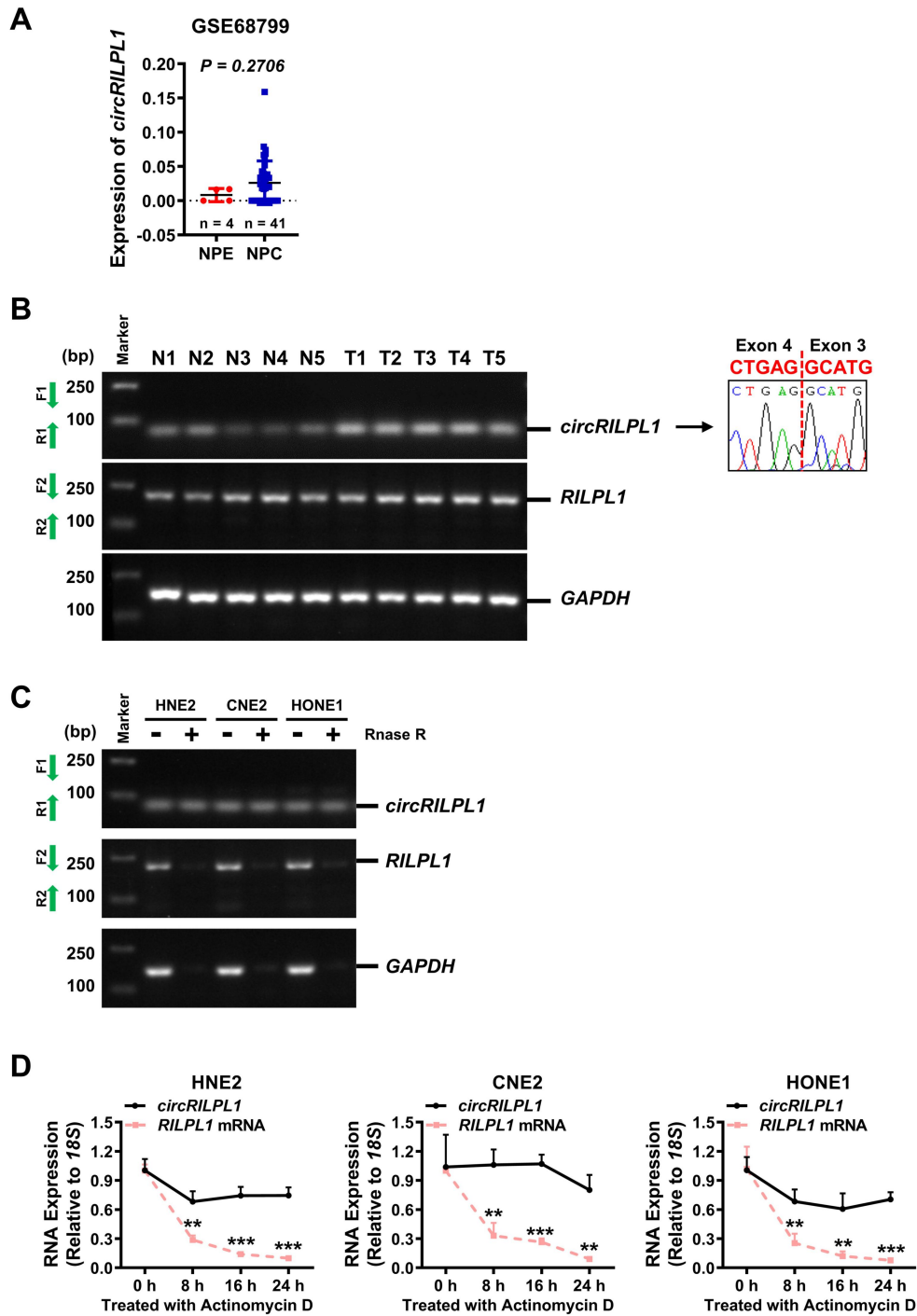


Fig. S1 CircRILPL1 is highly expressed in NPC tissues.

A. The expression levels of circRILPL1 in 41 NPC tissues and 4 NPE tissues in GSE68799, $p = 0.2706$. **B.** Gel figures of qRT-PCR results from representative tissue samples for the detection of circRILPL1 expression. Sanger sequencing was used to confirm the presence of circRILPL1. The linear RILPL1 mRNA and GAPDH mRNA were used as negative controls. **C.** Gel figures of qRT-PCR results showing the expression levels of circRILPL1 and RILPL1 mRNA in RNase R-treated NPC cells. GAPDH was used as an internal control. **D.** The relative expression levels of circRILPL1 and RILPL1 mRNA in NPC cells were detected after treating with actinomycin D for 0 h, 8 h, 16 h, and 24 h. 18S RNA was used as an internal reference. Data are presented as the means \pm SD. $**p < 0.01$, $***p < 0.001$.

Fig. S2

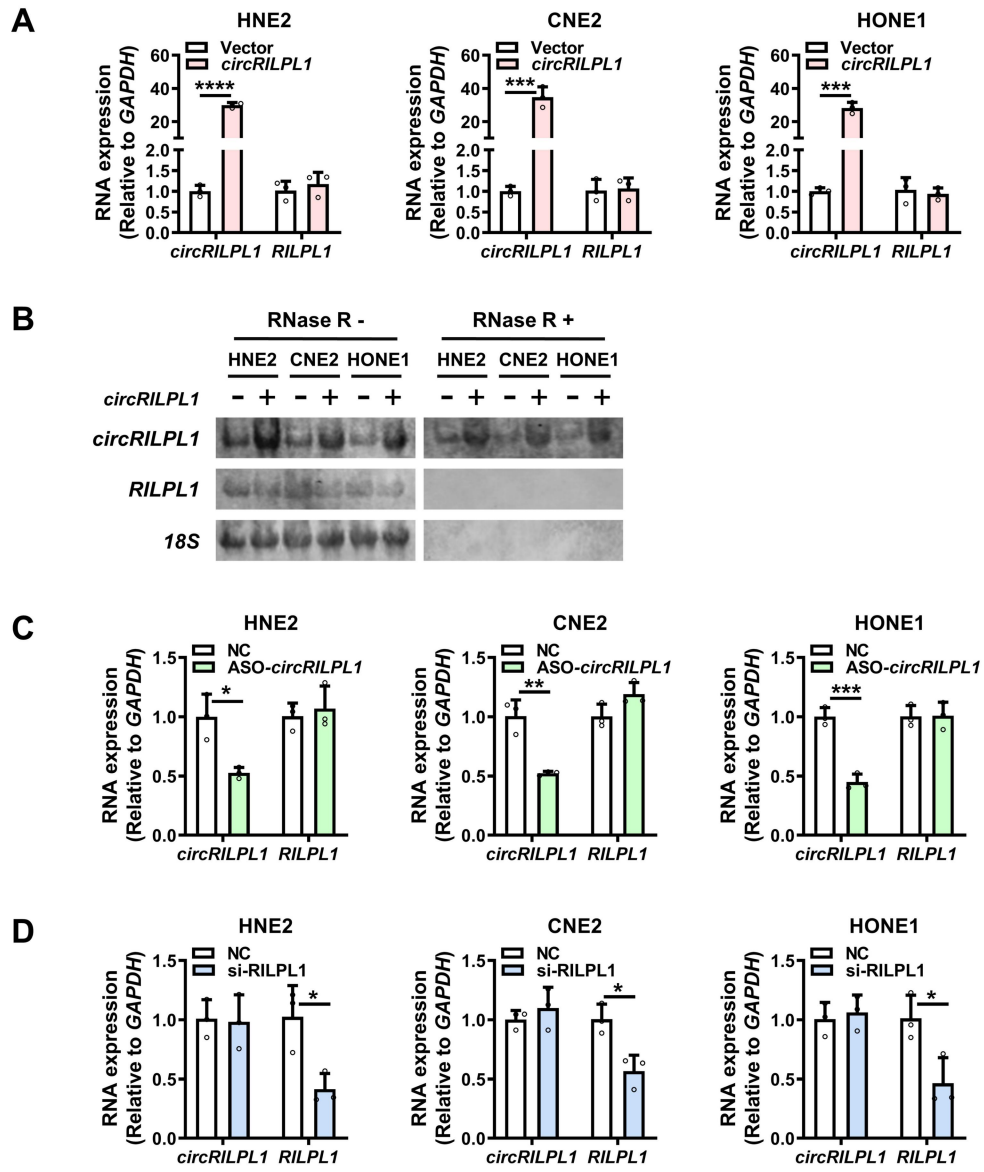


Fig. S2 CircRILPL1 perturbation did not affect the expression of RILPL1 and vice versa.

A. The expression of circRILPL1 was measured in HNE2, CNE2 and HONE1 cells after transfection with the circRILPL1 overexpression vector or empty vector. RILPL1 expression was not affected after overexpression of circRILPL1. **B.** Northern blotting analysis of circRILPL1 expression in NPC cells transfected with empty vector or circRILPL1 overexpressing plasmid with or without RNase R treatment. CircRILPL1 was probed using an oligonucleotide targeting the backsplice junction. RILPL1 mRNA was detected using RILPL1 specific probe. 18S RNA was used as a loading control. **C.** The expression of circRILPL1 was measured in HNE2, CNE2 and HONE1 cells after transfection with the circRILPL1 ASO or scramble negative control. RILPL1 expression was not affected after knockdown of circRILPL1. **D.** The expression of circRILPL1 was not affected after RILPL1 knockdown examined by qRT-PCR in NPC cells. Data are presented as the means \pm SD. * $p < 0.05$, ** $p < 0.01$, *** $p < 0.001$, **** $p < 0.0001$.

Fig. S3

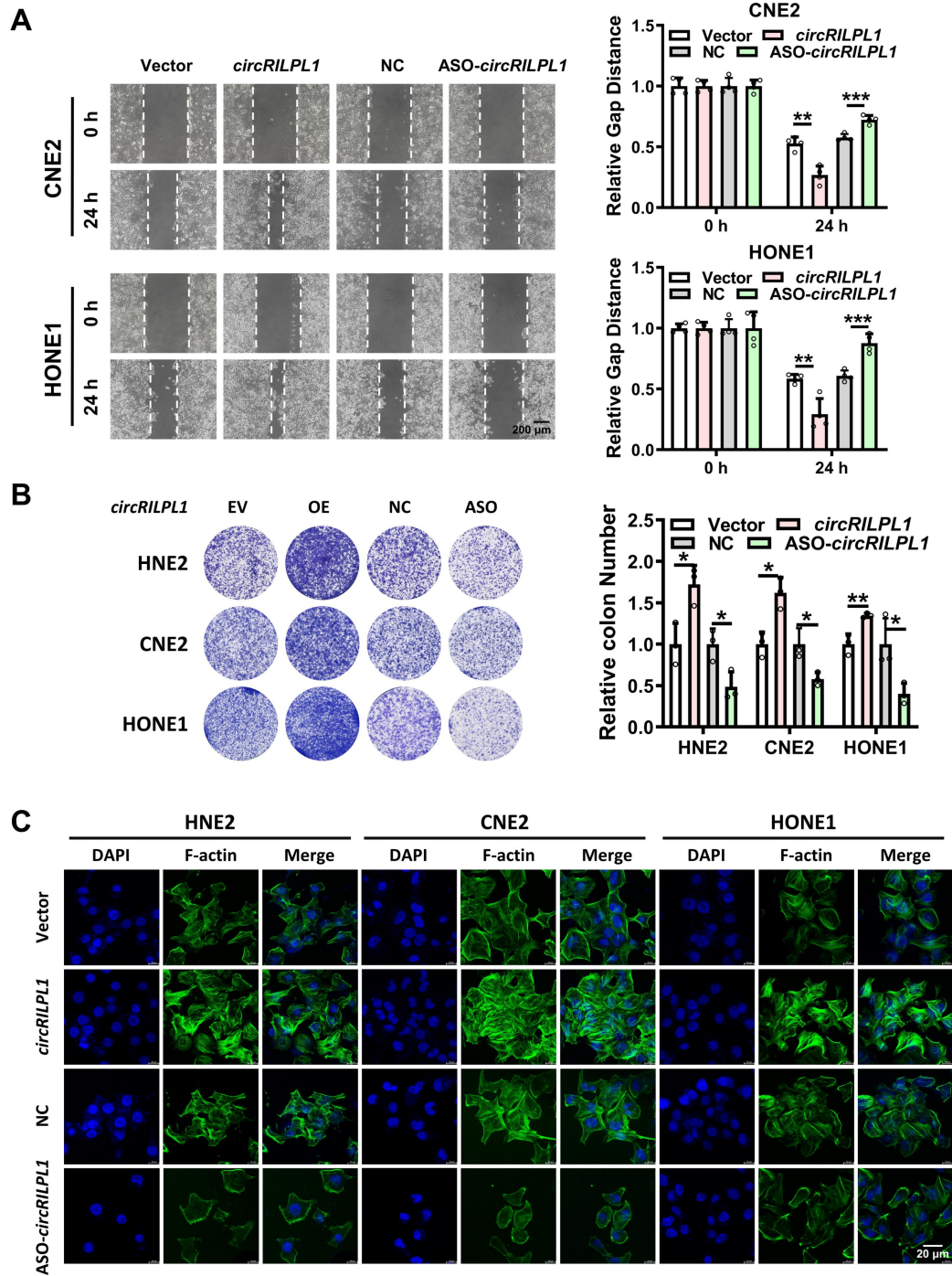
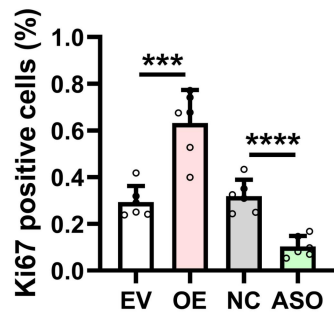


Fig. S3 CircRILPL1 promotes NPC cells migration, invasion, proliferation and alters the mechanical properties of NPC cells *in vitro*.

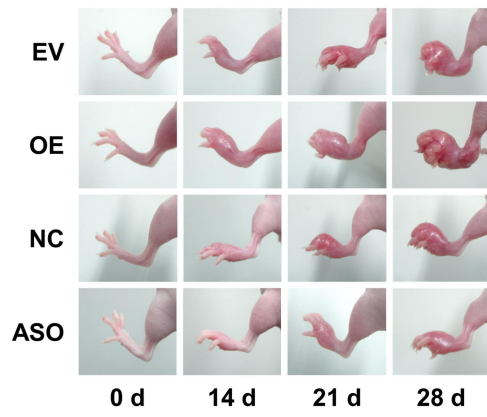
A. The migration ability of circRILPL1 in CNE2 and HONE1 was examined by wound healing assay. Images were acquired at 0 h and 24 h. Scale bars = 200 μm . **B.** The effect of circRILPL1 on NPC cells proliferation was evaluated by colon formation assays after overexpression or knockdown of circRILPL1. **C.** The effect of circRILPL1 on the formation of actin filaments was detected by immunofluorescence assay using phalloidin-labeled F-actin in NPC cells. DAPI: blue; F-actin: green; Scale bars = 20 μm . All data were presented as the means \pm SD. * $p < 0.05$, ** $p < 0.01$, *** $p < 0.001$.

Fig. S4

A



B



C

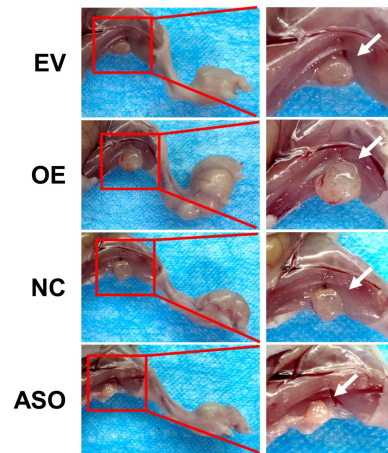


Fig. S4 CircRILPL1 promotes the proliferation and metastasis of NPC cells *in vivo*.

A. The percentage of Ki67 positive cells was quantified for each group. Data are presented as the means \pm SD. *** $p < 0.001$, **** $p < 0.0001$. **B.** Representative images of primary tumors at day 0, 14, 21 and 28 after CNE2 cells injection into the footpad of nude mice. **C.** The inguinal lymph nodes (white arrows) of nude mice were removed at day 28 for analysis.

Fig. S5

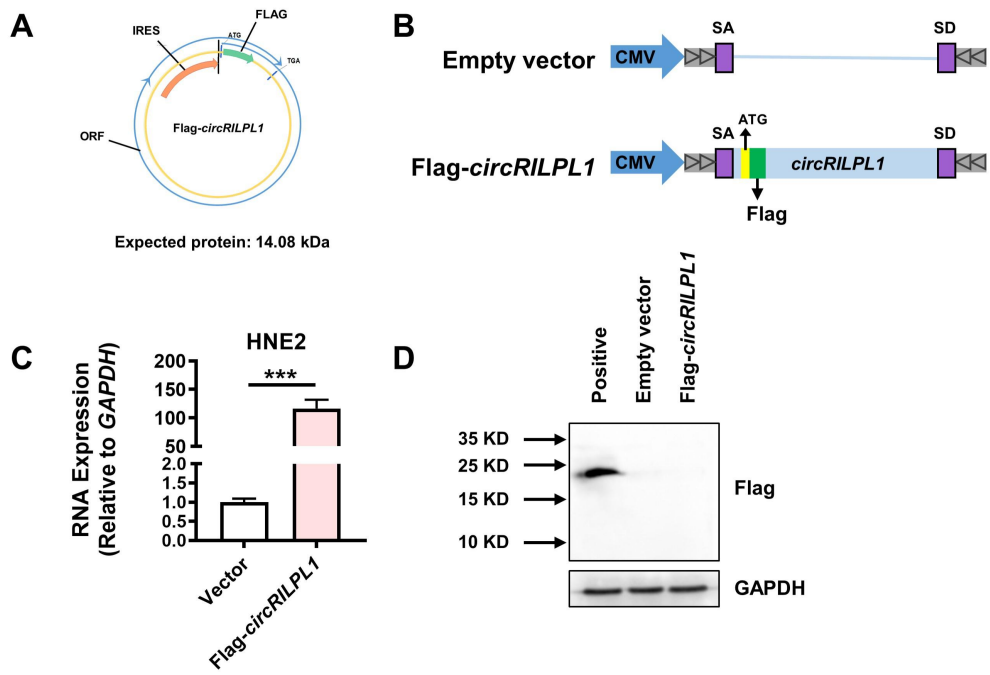
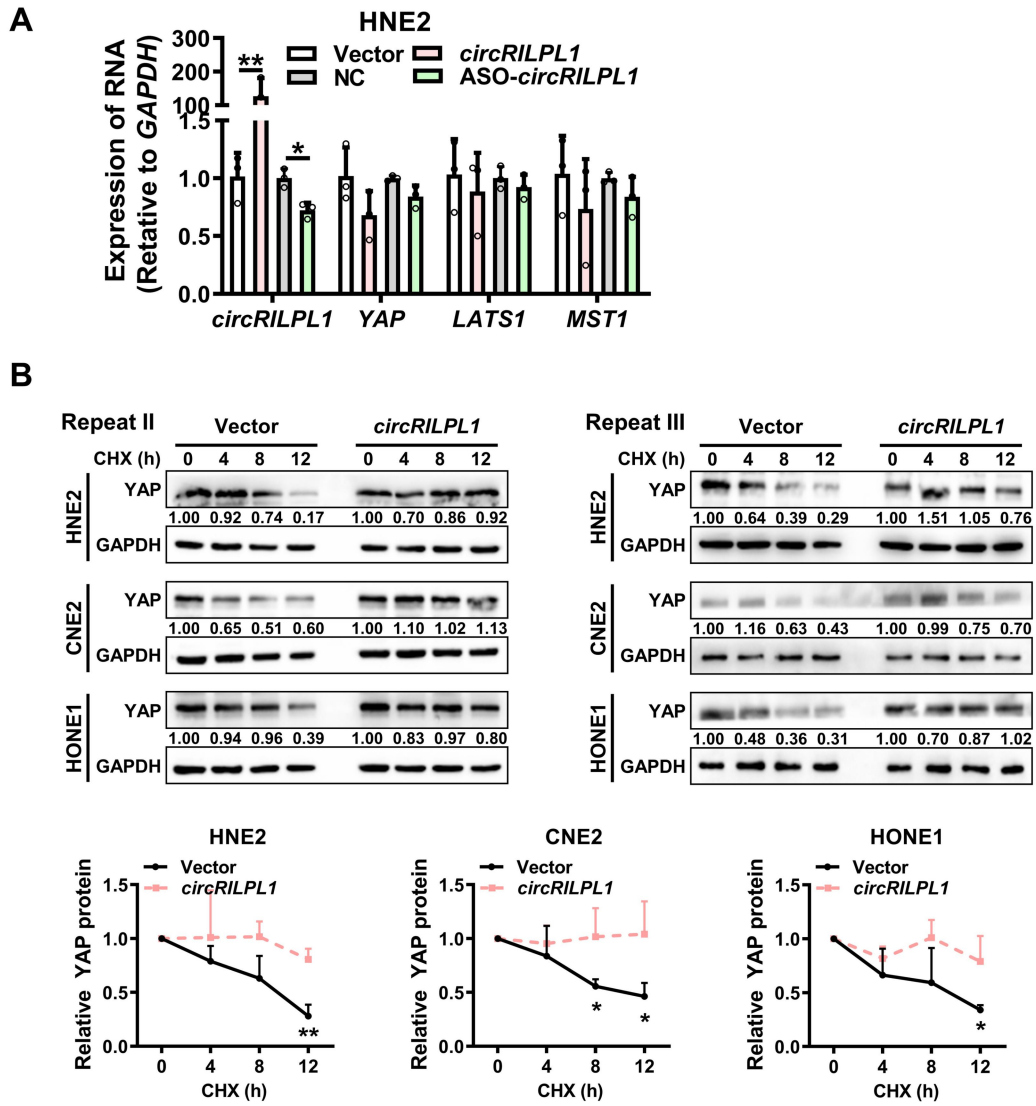


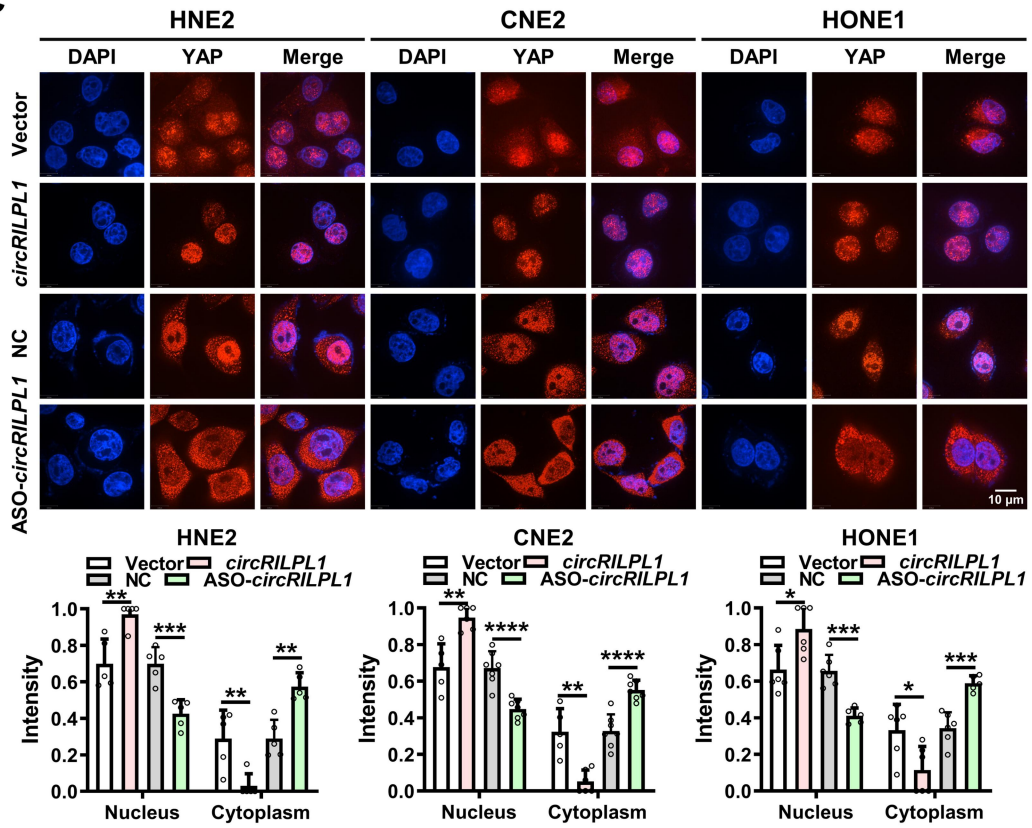
Fig. S5 CircRILPL1 could not encode peptides.

A. Schematic diagram of the Flag-circRILPL1 with ATG, TGA, ORF, IRES and Flag tag. Flag-circRILPL1 was expected to encode a small peptide of 14.08 KDa. **B.** Top: empty vector; Bottom: Flag-circRILPL1 overexpression vector, the sequence of circRILPL1 was cloned between the splice acceptor and splice donor, the Flag tag followed the ATG. **C.** The efficiencies of overexpression Flag-circRILPL1 were checked by qRT-PCR in HNE2 cells. Data are presented as the means \pm SD. *** $p < 0.001$. **D.** The expression was tested by western blot in HNE2 cells after transfection of empty vector and Flag-circRILPL1. The positive control is the Flag-tagged ANKRD14 protein (22.85 kDa).

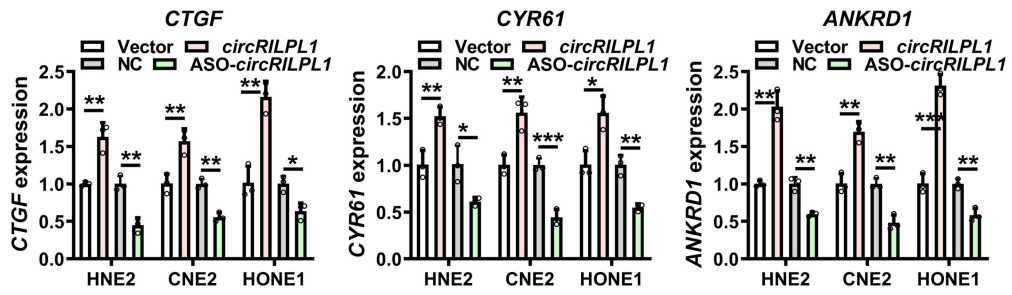
Fig. S6



C



D



E

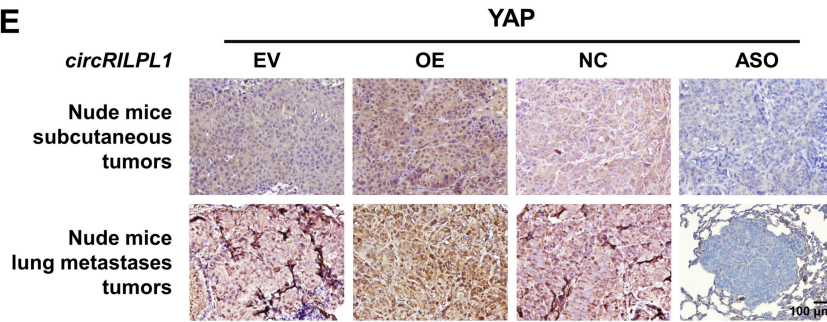
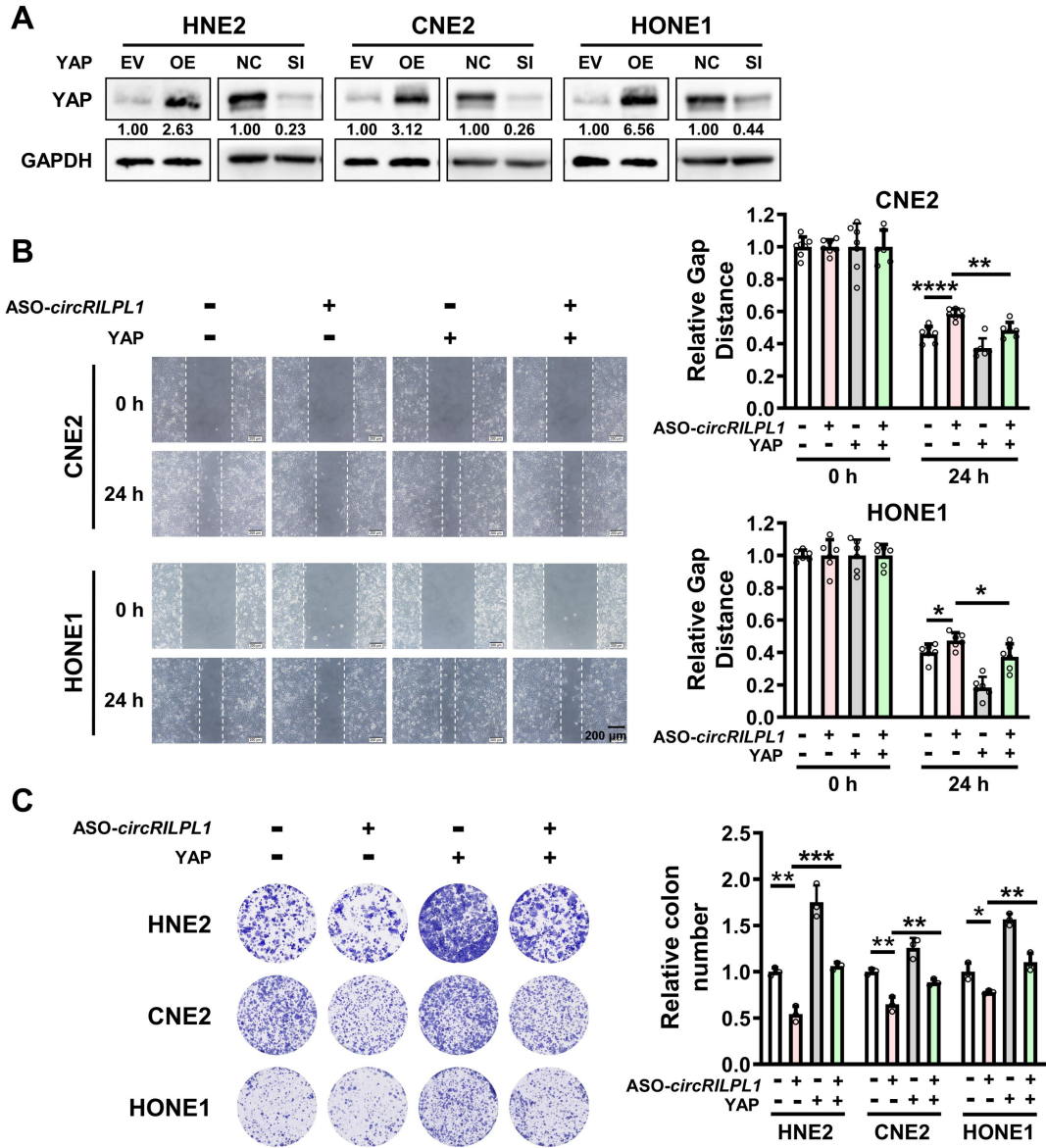


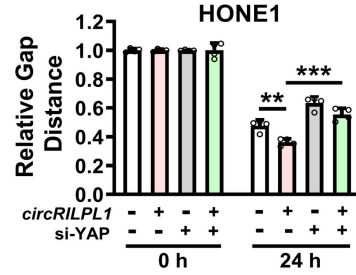
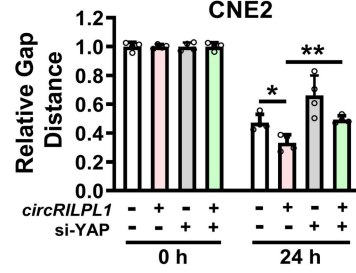
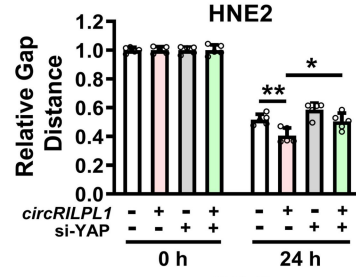
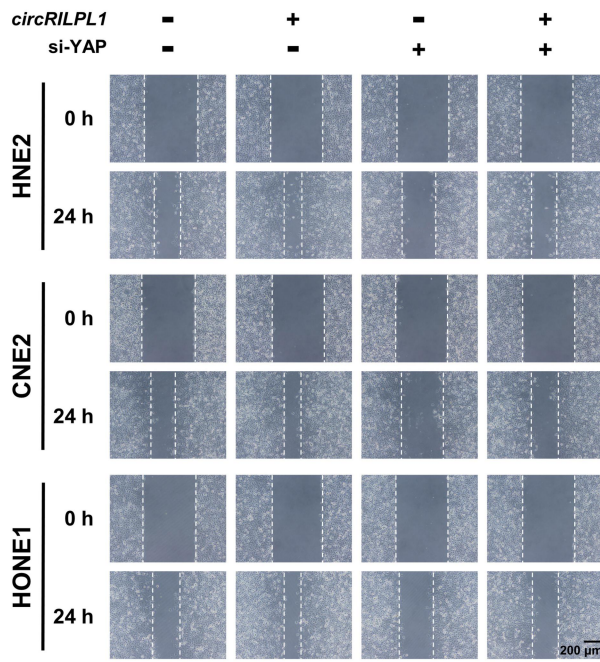
Fig. S6 CircRILPL1 activates the Hippo-YAP signaling pathway.

A. The effect of circRILPL1 on the mRNA expressions of key members of the Hippo signaling pathway were detected by qRT-PCR in HNE2 cells. **B.** The stability of YAP protein was measured in NPC cells after overexpression of circRILPL1. The degradation of YAP protein was determined by western blotting in NPC cells treated with cycloheximide (CHX, 50 $\mu\text{g}/\text{mL}$) for 0, 4, 8, 12 h after overexpression of circRILPL1. The experiments were repeated at three times. **C.** The effect of circRILPL1 on the subcellular localization of YAP was detected by immunofluorescence in NPC cells. DAPI: blue; YAP: red; Scale bar = 10 μm . **D.** The expression levels of CTGF, CYR61 and ANKRD1 mRNA were examined by qRT-PCR in NPC cells after overexpression or knockdown of circRILPL1. **E.** The expressions of YAP in nude mouse subcutaneous tumor model and lung metastasis model were detected by IHC. Scale bar = 100 μm . Data are presented as the means \pm SD. * $p < 0.05$, ** $p < 0.01$, *** $p < 0.001$, **** $p < 0.0001$.

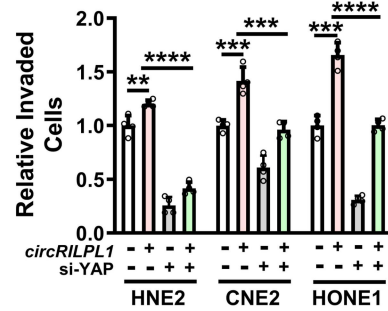
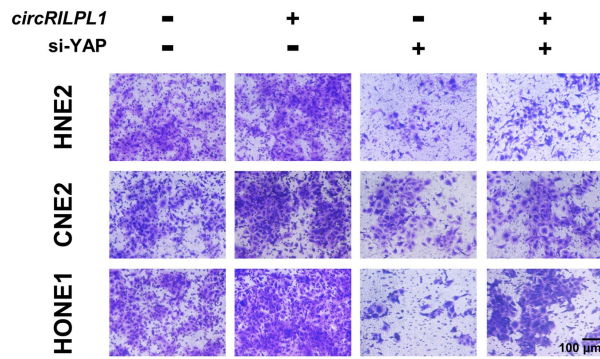
Fig. S7



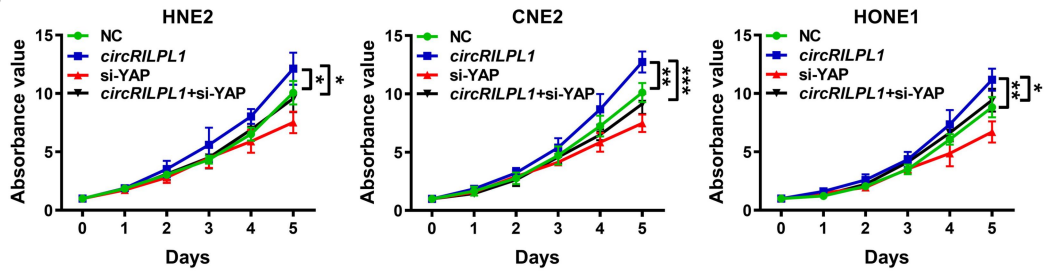
D



E



F



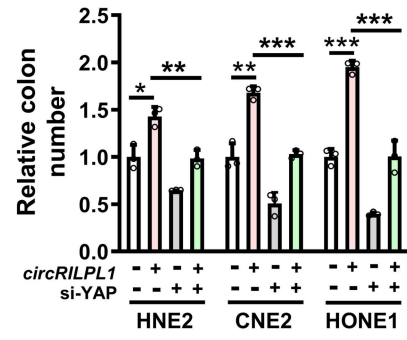
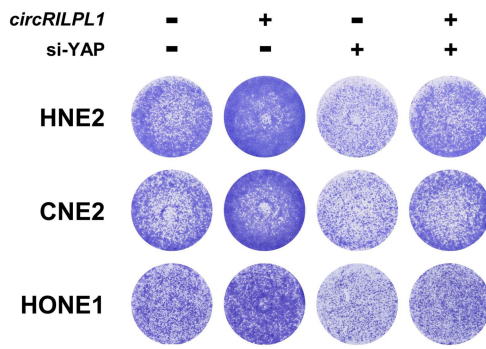
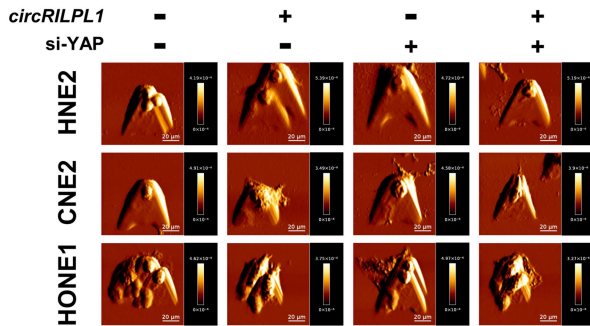
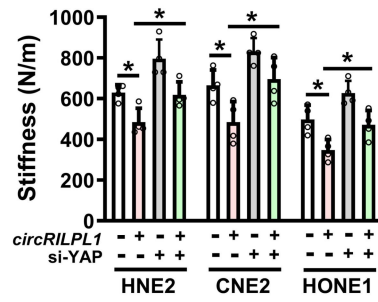
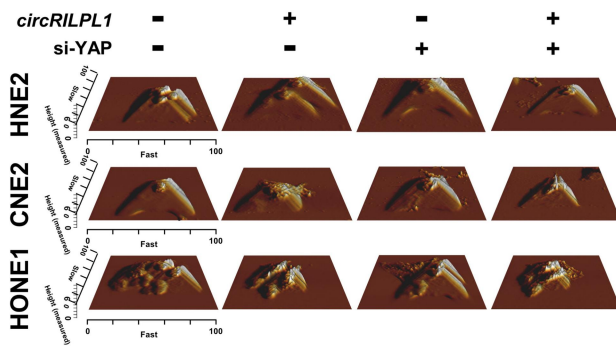
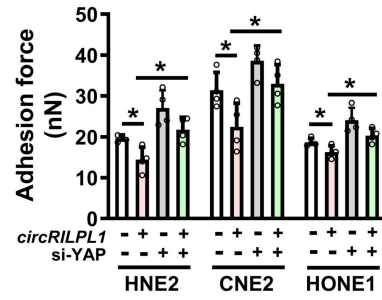
G**H****I****J****J**

Fig. S7 CircRILPL1 regulates NPC cells migration, invasion, proliferation and mechanical properties through YAP.

A. The overexpression or knockdown efficiencies of YAP protein were examined in NPC cells by western blotting. **B.** Wound healing assays showed that overexpression of YAP reversed the migration ability of circRILPL1 in CNE2 and HONE1 cells. Scale bars = 200 μ m. **C.** Colon formation assays showed that overexpression of YAP reversed the proliferation ability of circRILPL1 in NPC cells. **D-J.** The migration, invasion, proliferation and biophysical properties of NPC cells was examined by wound healing assays (**D**), transwell assays (**E**), MTT assays (**F**), colon formation assays(**G**) and AFM assays (**H-J**) after overexpression of circRILPL1 or knockdown of YAP. Data are presented as the means \pm SD.

* $p < 0.05$, ** $p < 0.01$, *** $p < 0.001$, **** $p < 0.0001$.

Fig. S8

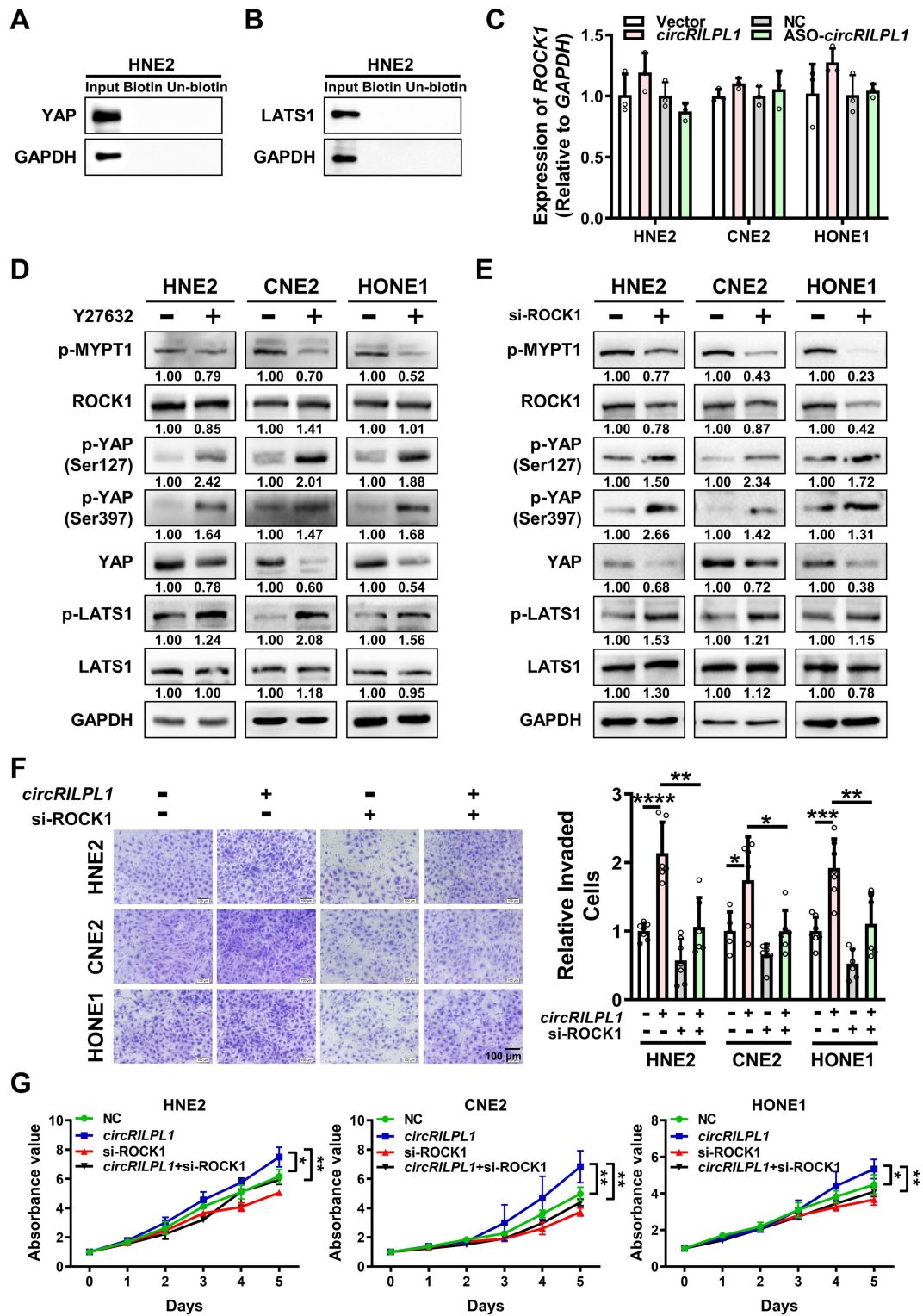
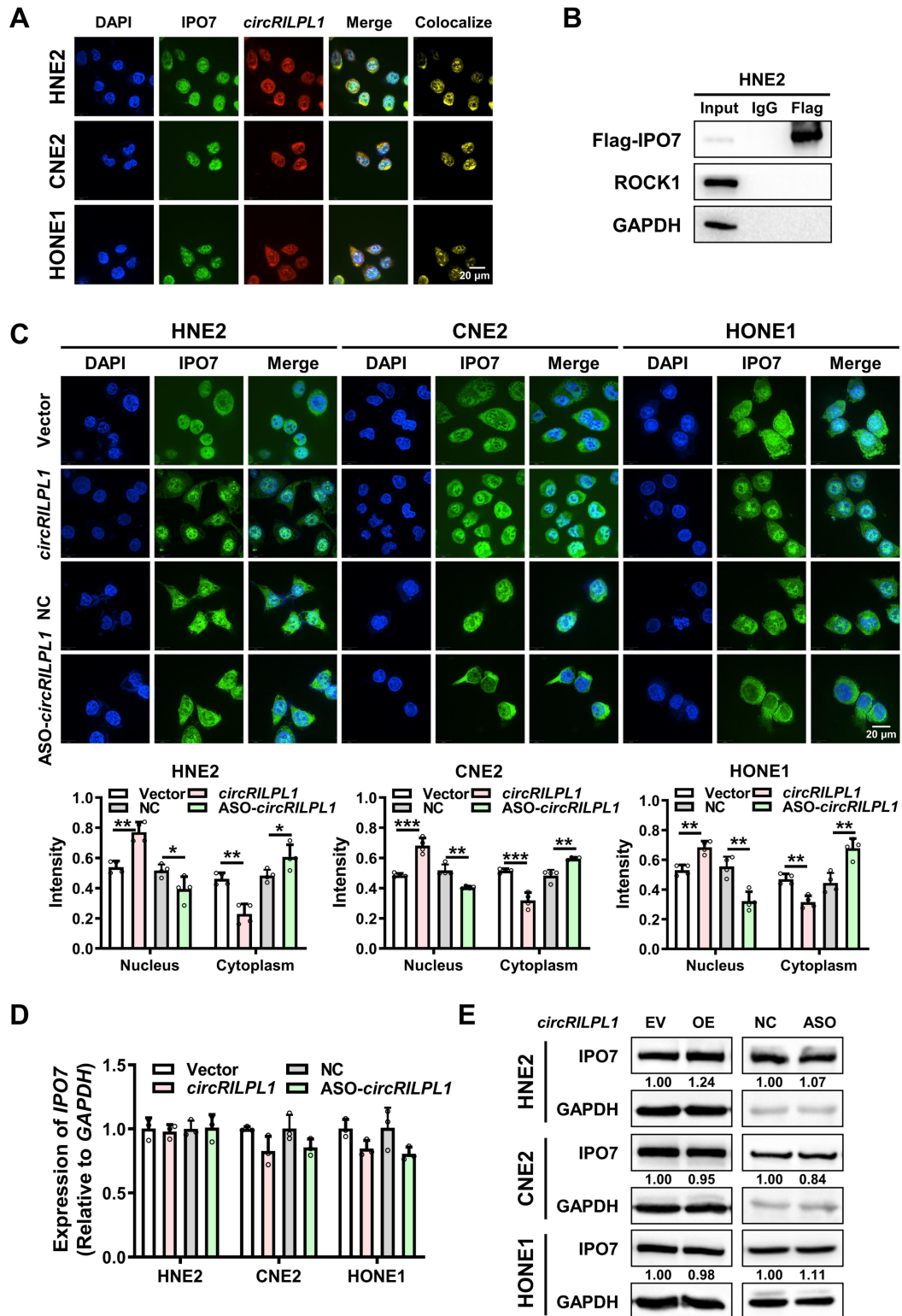


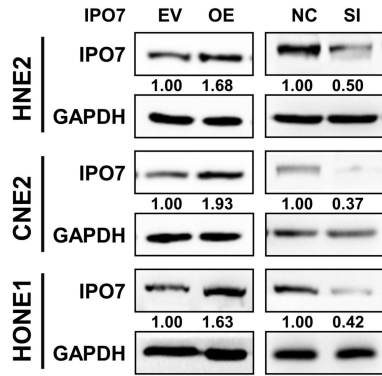
Fig. S8 CircRILPL1 relieves the LATS1-mediated YAP inhibition by binding to ROCK1.

A. RNA pull-down showed no binding between circRILPL1 and YAP protein in HNE2. GAPDH was used as a negative control. **B.** RNA pull-down showed no binding between circRILPL1 and LATS1 protein in HNE2. GAPDH was used as a negative control. **C.** The mRNA expression of ROCK1 was examined in NPC cells by qRT-PCR after overexpression or knockdown of circRILPL1. **D.** The expression of ROCK1, p-MYPT1 (Thr696), YAP, p-YAP ((Ser127 and Ser397), LATS1, p-LATS1 was analyzed in NPC cells by western blotting after treating with ROCK1 inhibitor Y27632 (10 uM) for 2 h. **E.** The expression of ROCK1, p-MYPT1 (Thr696), YAP, p-YAP (Ser127 and Ser397), LATS1, p-LATS1 was detected in NPC cells by western blotting after knockdown of ROCK1. **F.** The invasive ability of NPC cells was examined by Transwell assays after overexpression of circRILPL1 or knockdown of ROCK1. Scale bars = 100 μ m. **G.** The proliferation ability of NPC cells was measured by MTT assays after overexpression of circRILPL1 or knockdown of ROCK1. Data are presented as the means \pm SD. * $p < 0.05$, ** $p < 0.01$, *** $p < 0.001$, **** $p < 0.0001$.

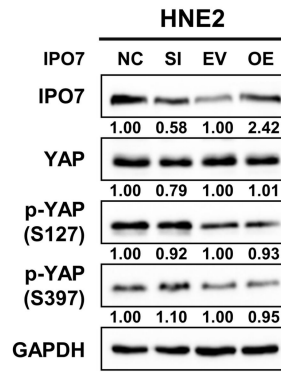
Fig. S9



F



G



H

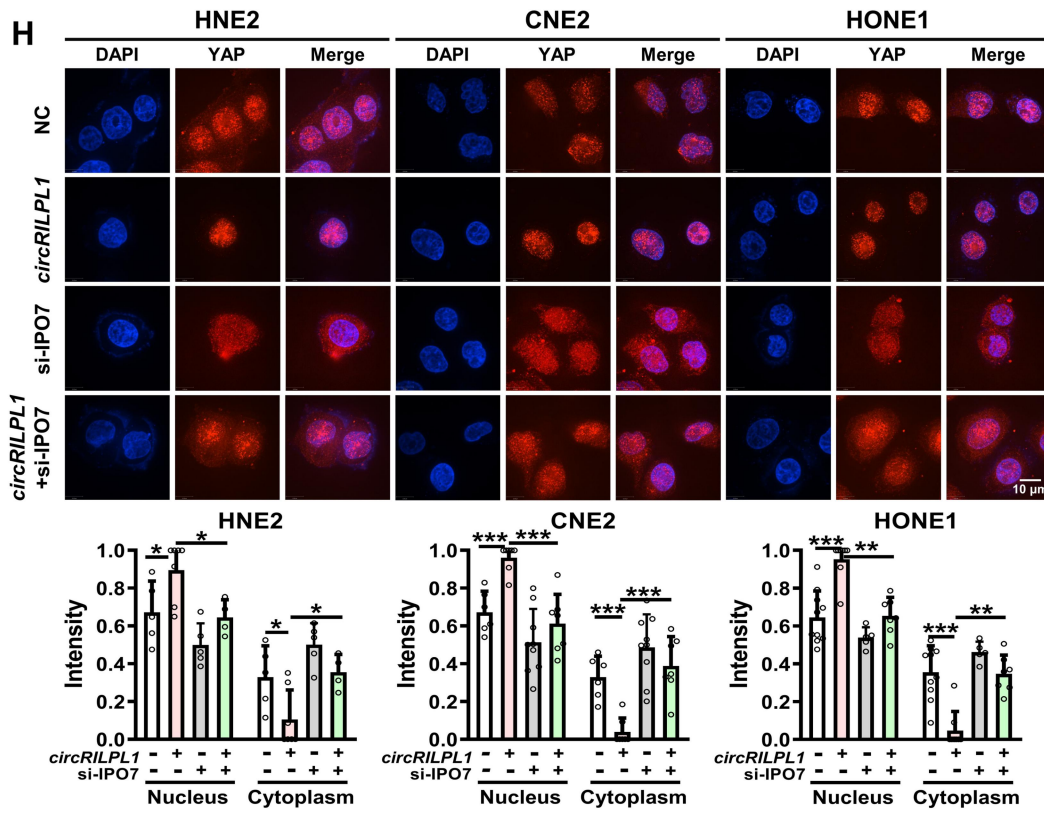


Fig. S9 CircRILPL1 promotes YAP nuclear translocation through enhancing the interaction between YAP and IPO7.

A. The co-localization between circRILPL1 and IPO7 was detected by IF-FISH. DAPI: blue; IPO7: green; CircRILPL1: red; Scale bar = 20 μm . **B.** No interaction between ROCK1 and IPO7 in HNE2 cells. GAPDH was used as a negative control. **C.** The subcellular localization of IPO7 was detected in NPC cells by immunofluorescence after overexpression or knockdown of circRILPL1. The statistical results of the nucleus/cytoplasm ratio were shown below, which are quantified by the ImageJ software. DAPI: blue; IPO7: green; Scale bar = 20 μm . **D.** The mRNA expression of IPO7 was examined in NPC cells by qRT-PCR after overexpression or knockdown of circRILPL1. **E.** The protein expression of IPO7 was examined by western blotting after overexpression or knockdown of circRILPL1. **F.** The efficiencies of overexpression or knockdown of IPO7 protein were examined by western blotting. **G.** Western blotting showed that IPO7 did not regulate the expression and phosphorylation level of YAP in HNE2 cells. **H.** IPO7 participated in circRILPL1-induced YAP translocation from cytoplasm into nucleus in NPC cells. DAPI: blue; YAP: red; Scale bar = 10 μm . Data are presented as the means \pm SD. * $p < 0.05$, ** $p < 0.01$, *** $p < 0.001$.

Fig. S10

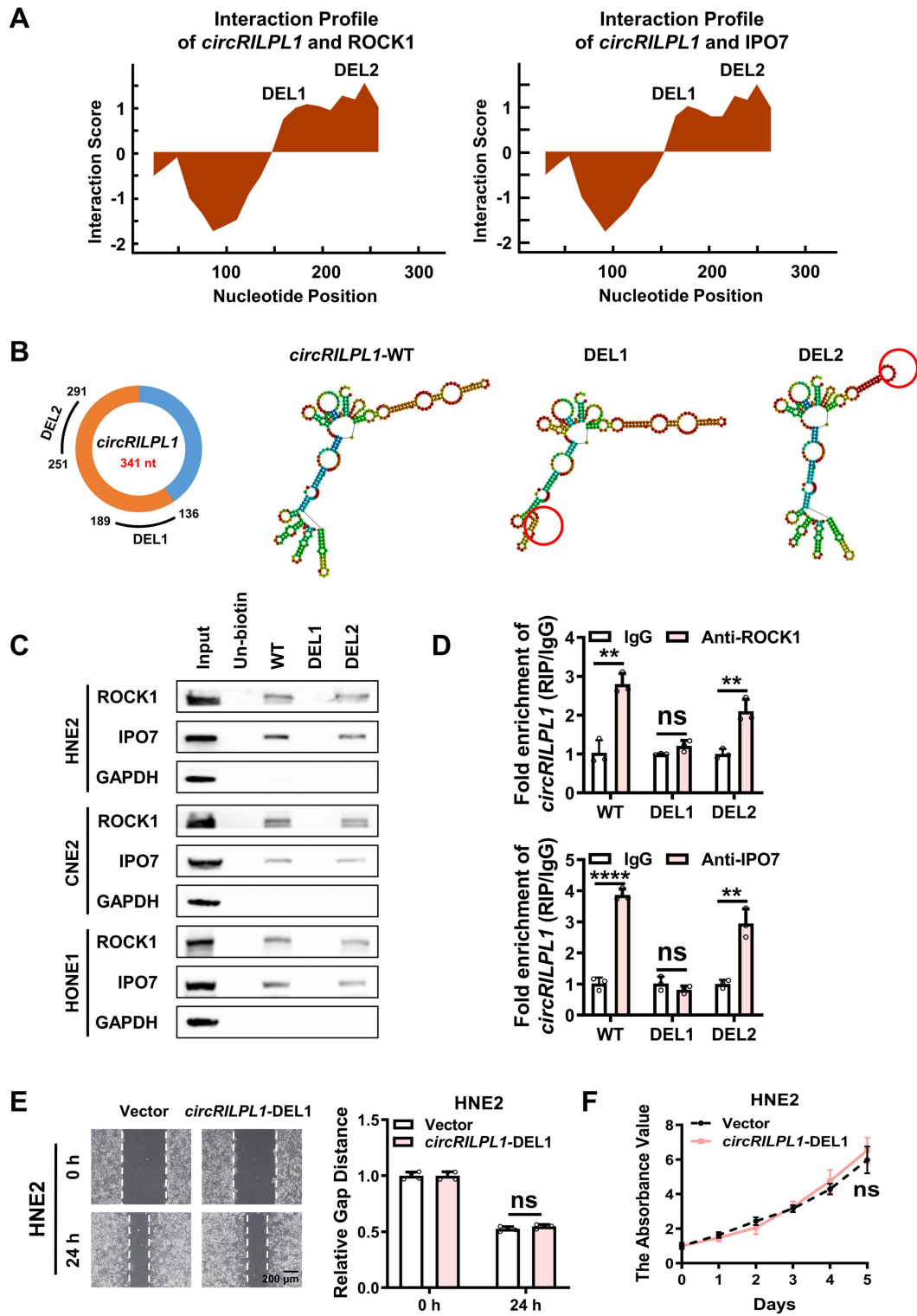


Fig. S10 CircRILPL1 interacts with ROCK1 and IPO7 through nucleotides 136-189.

A. ROCK1 and IPO7 were predicted to bind with the circRILPL1 sequence using the catRAPID software. **B.** Two well characterized stem loop structures (136-189 nt named DEL1, 251-291 nt named DEL2) were predicted on the circRILPL1 using the RNAfold database. **C.** The 136-189 nt of circRILPL1 was crucial for the binding between circRILPL1 with ROCK1 and IPO7 proteins. NPC cells were transfected with the full-length circRILPL1 (WT) or deletion mutants (DEL1 and DEL2). RNA pull-down assays were performed using the biotin-labeled circRILPL1 probe, followed by western blotting using anti-ROCK1 and anti-IPO7 antibody. GAPDH was used as a negative control. **D.** ROCK1 and IPO7 proteins directly bind to the 136-189 nt of circRILPL1. Cells were transfected with the full-length circRILPL1 (WT) or deletion mutants (DEL1 and DEL2). RNA immunoprecipitation was performed using anti-ROCK1 and anti-IPO7, followed by qRT-PCR analysis for circRILPL1. **E.** The effect of deletion mutant circRILPL1-DEL1 on the migration ability of HNE2 cells examined by wound healing assay. **F.** The effect of deletion mutant circRILPL1-DEL1 on the proliferation ability of HNE2 cells examined by MTT assay. Data are presented as the means \pm SD. NS, not significant. ** $p < 0.01$, **** $p < 0.0001$.

Fig. S11

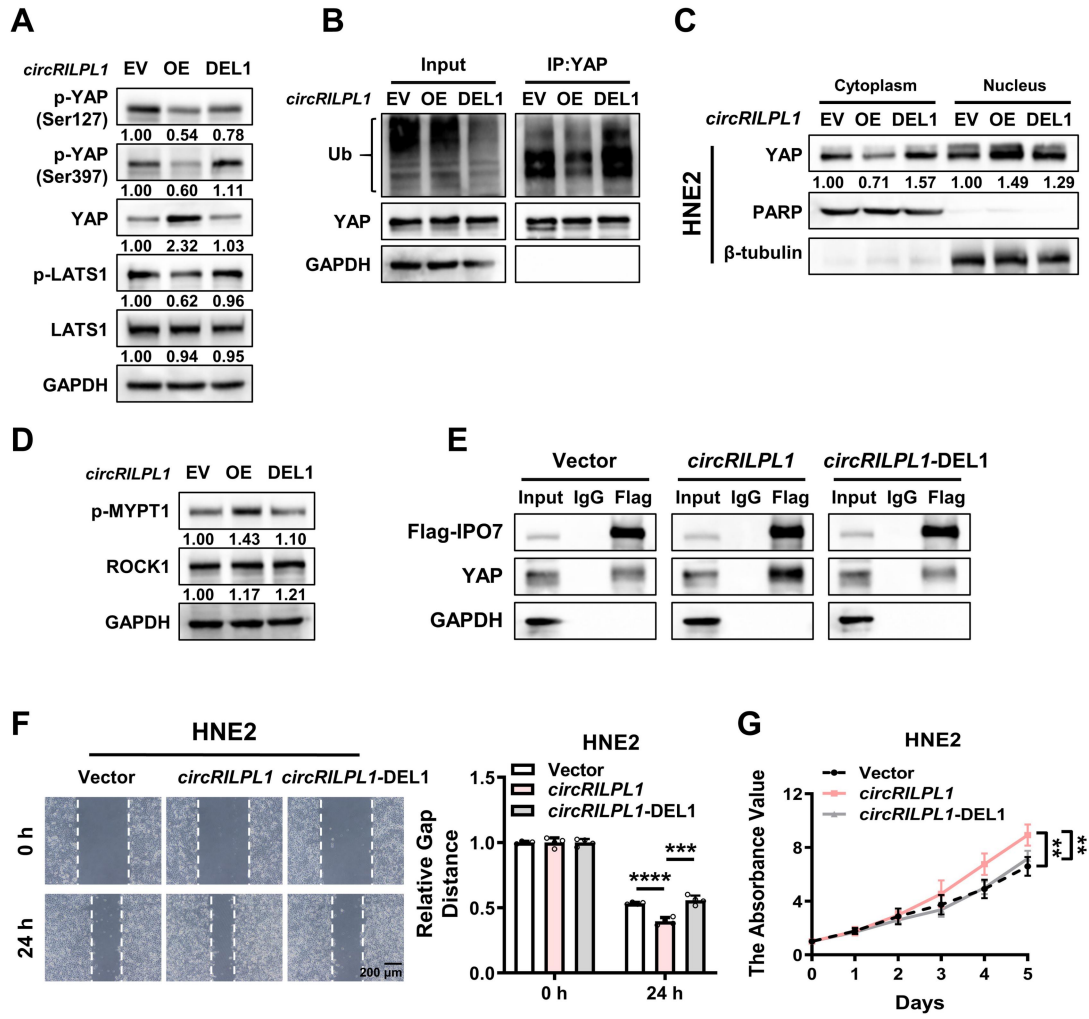


Fig. S11 Nucleotides 136-189 is critical for circRILPL1 to regulate YAP activation and promote NPC cells migration and proliferation.

A. The effects of wild-type circRILPL1 or the mutant circRILPL1-DEL1(136-189 nt deleted) on the expression level of key proteins of the Hippo signaling pathway were determined by western blotting in HNE2 cells. **B.** The effect of wild-type circRILPL1 or the mutant circRILPL1-DEL1 on the ubiquitination level of YAP protein was measured immunoprecipitation and western blotting assay in HNE2 cells treated with MG132 for 12 h. Cell lysates were subjected to immunoprecipitation using anti-YAP antibody followed by western blotting using anti-ubiquitin antibody. **C.** The abundance of YAP protein in nucleus and cytoplasm was examined in HNE2 cells after overexpression of circRILPL1 or circRILPL1-DEL1. PARP was used as a loading control for nuclear protein, whereas β -tubulin was used as a loading control for cytoplasmic protein. **D.** The effects of wild-type circRILPL1 or circRILPL1-DEL1 on MYPT1 (Thr696) phosphorylation and ROCK1 protein were measured by western blotting in HNE2 cells. **E.** The effect of circRILPL1 or circRILPL1-DEL1 on the interaction between YAP and IPO7 was measured by immunoprecipitation using anti-Flag (IPO7) antibody, followed by western blotting using YAP antibody in HNE2 cells. GAPDH was used as a negative control. **F.** Wound healing assays showed that circRILPL1 but not the mutant (circRILPL1-DEL1) enhanced the migration abilities of HNE2 cells. **G.** MTT assays showed that circRILPL1, rather than circRILPL1-DEL1, promoted the proliferation of HNE2 cells. Data were represented as mean \pm SD. ** $p < 0.01$, *** $p < 0.001$, **** $p < 0.0001$.

Fig. S12

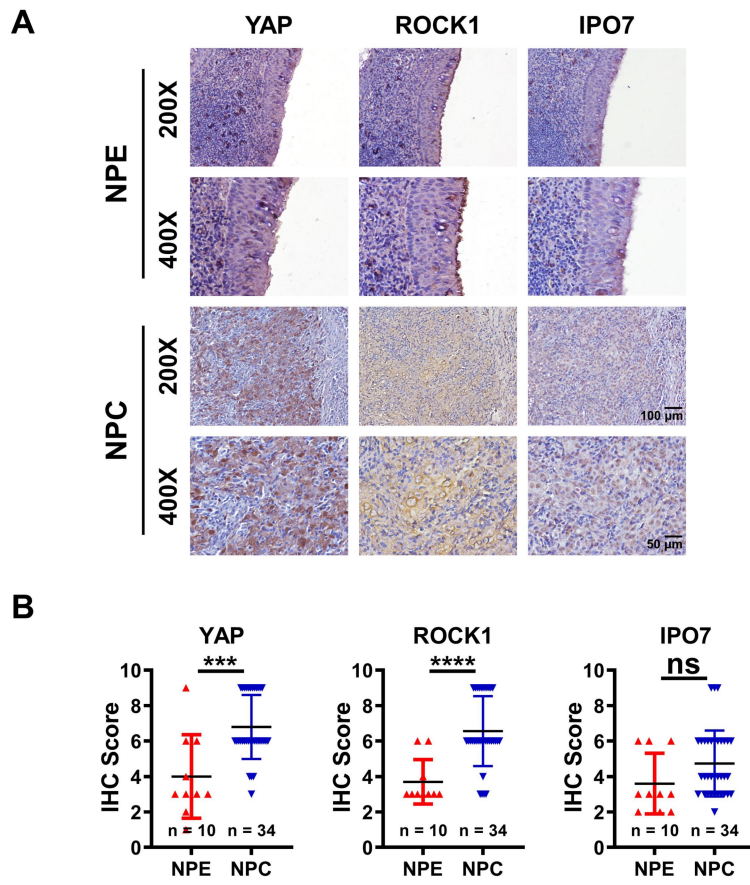


Fig. S12 YAP and ROCK1 are significantly highly expressed in NPC tissues

A. Immunohistochemistry was performed to detect the expression of YAP, ROCK1 and IPO7 in 10 NPE tissues and 34 NPC tissues. Magnification: 200×, Scale bar = 100 μm; Magnification: 400×, Scale bar = 50 μm. **B.** The statistical results of YAP, ROCK1, and IPO7 expression in 10 NPE and 34 NPC tissues. Data are presented as the means ± SD. NS, not significant. *** $p < 0.001$, **** $p < 0.0001$.

Fig. S13

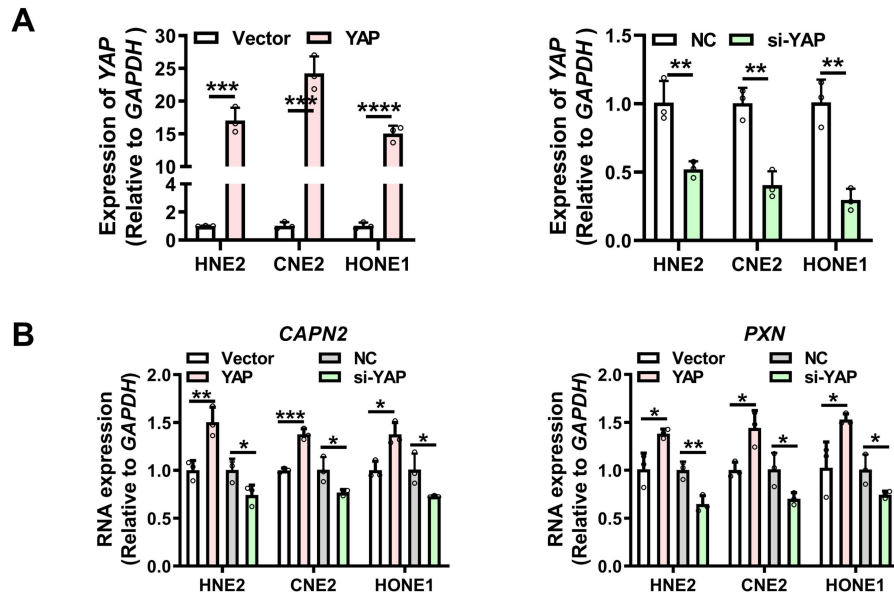


Fig. S13 CircRILPL1-YAP signaling promotes the transcription of CAPN2 and PXN.

A. The efficiencies of overexpression and knockdown of YAP were examined in NPC cells by qRT-PCR. **B.** The mRNA expression of CAPN2 and PXN was examined by qRT-PCR after overexpression or knockdown of YAP in NPC cells. Data are presented as the means \pm SD. * p < 0.05, ** p < 0.01, *** p < 0.001, **** p < 0.0001.

Supplemental Table 1. 30 circRNAs up-regulated in NPC tissues identified in the GSE68799 dataset.

Supplemental Table 2. Proteomic analysis of the circRILPL1-regulated proteins in HNE2 cells by LC-MS/MS spectrometry.

Supplemental Table 3. Proteins in mass spectrometry dataset are enriched in the Hippo signaling pathway.

Supplemental Table 4. Proteins identified after pull-down with biotin-labeled circRILPL1 probe.

Supplemental Table 5. Proteins upregulated by circRILPL1 and involved in cell adhesion junctions and cytoskeleton remodeling pathways in mass spectrometry.

Supplemental Table 6. Clinicopathological data for 38 NPC and 16 NPE tissues-used for qRT-PCR.

Supplementary Table 7. Clinicopathological data for 99 paraffin-embedded NPC tissues used for *in situ* hybridization.

Supplemental Table 8. Probes for ISH, RNA pull-down, and siRNAs; and primers for qRT-PCR and cloning.

Supplemental Table 9. List of antibodies for western blotting, immunohistochemistry, immunofluorescence, RNA pull-down, and RIP experiment.